

Real and Imaginary Elements of Fermion Mass Matrices

I. Masina^a and C.A. Savoy^b

*a) Centro Studi e Ricerche "E. Fermi", Via Panisperna 89/A, Rome, Italy
and INFN, Sezione di Roma, P.le A. Moro 2, Rome, Italy*
b) Service de Physique Théorique, CEA-Saclay, Gif-sur-Yvette, France

Abstract

Prompted by the recent better determination of the angles of the unitarity triangle, we re-appraise the problem of finding simple fermion mass textures, possibly linked to some symmetry principle and compatible with grand unification. In particular, the indication that the angle α is close to rectangle turns out to be the crucial ingredient leading us to single out fermion mass textures whose elements are either real or purely imaginary. In terms of the five parameters ascribed to the quark sector, these textures reproduce the eight experimental data on quark mass ratios and mixings within 1σ . When embedded in an $SU(5)$ framework, these textures suggest a common origin for quark and lepton CP violations, also linked to the spontaneous breaking of the gauge group.

”Perche’, secondo l’opinion mia, a chi vuole una cosa ritrovare, bisogna adoperar la fantasia, e giocar d’invenzione, e ’ndovinare.¹” (Galileo Galilei)

1 Introduction

In this work, we reconsider the problem of finding simple textures, which could possibly be linked to some symmetry principle or simply embedded in a grand unification context. In practice, we have to write two quark mass matrices consistent with the ten experimental observables (six mass eigenvalues, three angles and one phase of the CKM mixing matrix) in terms of as few parameters as possible, by establishing simple relations between observables to make the model predictive.

Since the Gatto-Sartori-Tonin (GST) relation $\sin \theta_C \approx \sqrt{m_d/m_s}$ was pointed out [1], a lot of mass matrix models generalized it to three generations (see e.g. [2]–[12]). Yet, the more and more precise experimental data have ruled out or disfavored many interesting fermion mass textures proposed so far. For instance, the pioneering ones proposed by Georgi and Jarlskog (GJ) [3] do not satisfy the V_{cb} constraint since 16 years [4] and, thanks to the increased sensitivities to $|V_{ub}/V_{cb}|$ and $\sin \beta$, also the more general class of symmetric textures with zeros in the 11,13 and 31 elements [5] has turned out to be disfavored [8, 9, 10, 11].

Recently, an interesting phenomenological fact has been emerging, whose impact on fermion mass matrices deserves proper consideration. As suggested both from direct measurements [13] and global CKM fits [14]², the unitarity triangle is rectangle or nearly so: $\alpha \sim 90^\circ$. Since $\sin \alpha = \sin \beta / R_u$, this can be easily realized for global fits by comparing the smallest side of the unitarity triangle, $R_u = |\frac{V_{ud}V_{ub}}{V_{cd}V_{cb}}|$, with the precisely measured angle in front of it, β . We draw such a comparison in fig. 1, also showing how much the robustness of $\alpha \sim 90^\circ$ has increased during the last years.

After introducing our notations and conventions in Section 2, we analyse in Section 3 the simplest possibility that near-neighbor-generation mixings are given in terms of the four ratios of quark masses, while far-neighbor-generation mixings vanish. A very important role is played by the non-removable phases between left-chirality families, which are a potential source of CP violation (CPV) [5, 7, 12, 16]. To avoid to introduce new parameters, the simplest approach is to assume that these phases are either $0, \pm\pi/2$ or π , namely that such sources of CPV are either maximal or switched off. It is known that the presence of a maximal phase between two quarks or two leptons of left-chirality has

¹From *Capitolo contro il portar la toga* in ”Dialogo sopra i due Massimi Sistemi del Mondo Tolemaico e Coperniano” (1632).

²As the results of the fits carried out by different collaborations [14, 15] agree, in this work we adopt for definiteness the fit of ref. [14].

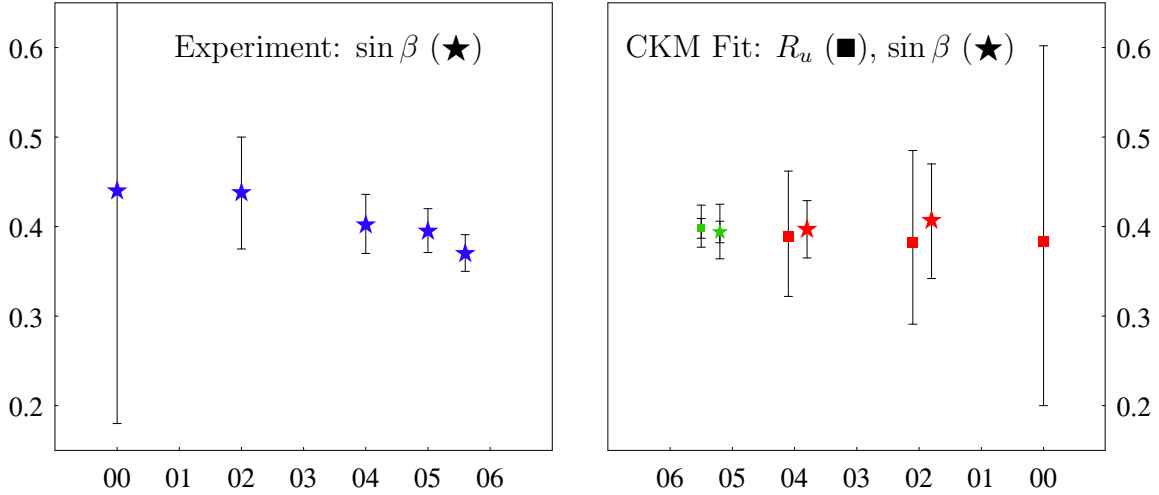


Figure 1: Left: experimental value of $\sin \beta$ [17]: average measurements from BaBar and Belle since 2002; CDF results for year 2000. Right: CKM fit value of R_u and $\sin \beta$ according to: the Particle Data Group (PDG) [17] at 90% c.l. from 2000 to 2004; CKMfitter Collaboration [14] at 1 and 2σ after summer 2005.

important consequences: $\sin \theta_C$ is numerically so close to $\sqrt{m_d/m_s}$ that a maximal phase between the lightest generations of quarks is needed to preserve the GST relation from corrections due to the up-quark sector [7, 8, 9]; a maximal phase between the μ and τ leptons permits to end up with a maximal atmospheric angle, starting from a $\pi/4$ mixing in the $\nu_\mu - \nu_\tau$ and/or $\mu - \tau$ sectors [16]. As we are going to argue, a maximal phase between the heaviest generations of quarks or between the e and μ leptons is instead not suitable respectively for $|V_{cb}|$ and the solar angle³.

Following the guidelines so obtained, we are lead to write down a simple set of quark mass matrices, eq. (14), whose elements are real but for a purely imaginary one and simply depend on quark mass ratios. The up-quark mass matrix \mathbf{m}_u has a double seesaw-like (or Fritzsch [2]) form; together with \mathbf{m}_d , these textures can be viewed as a renewed version of the GJ ones. This predictive set belongs to the category of the so-called "5 zero" textures and gives a quite reasonable fit of the quark masses and the CKM mixing matrix, with the specific prediction $\alpha \approx \pi/2$. The weak point is that, in order to fit β and $|V_{ub}/V_{cb}|$, the up-quark mass comes out too large as compared to the chiral perturbation theory (CPT) result [19]. This is the same problem which has been pointed out, though with different approaches, in refs. [8, 9, 11, 12].

We then consider introducing additional small parameters that could make the agree-

³For attempts to obtain the solar angle by exploiting a maximal CPV phase between the e and μ leptons see ref. [18].

ment with data more satisfactory and identify the best choice to cure this problem. We show that switching on far-neighbor mixings to fit β and $|V_{ub}/V_{cb}|$ would correspondingly deteriorate the fit of α , which would now be missed by about 2σ . This remedy was adopted in refs. [9, 11, 12] (from their perspective, filling the zero in the 31-element of \mathbf{m}_d), when the much poorer sensitivity to α could not reveal a conflict. Driven by the recent data, we abandon that way and rather adopt a remedy which does not alter the desirable prediction $\alpha \approx \pi/2$, allowing for vanishing far-neighbor mixings. It consists in simply giving up the strict dependence on mass ratios involving the up-quark mass by the introduction of a small parameter in the 11-element of \mathbf{m}_u .

Inspired by the analysis in Section 3, in Section 4 we carry out a more general analysis by studying quark textures with 10 parameters and 6 possibly relevant phases. We show how experimental data single out two sets of quark textures with real or imaginary elements and which depend only on 5 parameters. The analysis proves that these two sets of textures, among which is the one obtained from the educated guess of Section 3, are stable solutions in the face of experimental data. Textures are of course defined up to unitary transformations that leave the CKM matrix invariant⁴, however only unitary transformations that do not introduce new small parameters - namely those that correspond to rotation angles and phases which are $0, \pm\pi/2, \pi$ - would meet our requirements. Indeed, it turns out that the down-quark textures of the two sets are related by a unitary transformation acting on the right-handed down-quarks which has only one maximal angle and maximal phases.

The previous results concern fermion mass textures at the electro-weak scale. There are two, non-independent reasons to transpose our analysis to the grand unification scale: 1) the extension of the analysis to the lepton sector becomes more predictive in a GUT framework; 2) $\Lambda \geq M_{GUT}$ is a natural scale to define broken flavour symmetries capable to explain the mass textures. Of course the data fitting must now take into account the running of the textures down to the electro-weak scale, as done in Section 5. This evolution modifies the imposed relations among the parameters. If only the top coupling is large (small $\tan\beta$), the agreement with data is fair, but including the contributions from the bottom and τ couplings (large $\tan\beta$) the agreement is further improved.

In Section 6, we embed the proposed textures in an $SU(5)$ GUT framework [20]. The Yukawa couplings in the mass matrices cannot all transform as $SU(5)$ singlets, because the invariance of the Yukawa matrices would lead to the prediction $m_e^T = m_d$, in contrast with the more realistic GJ relations $m_b = m_\tau$, $3m_s = m_\mu$, $m_d = 3m_e$ [3]. In general these couplings depend on the v.e.v.'s that break $SU(5)$ in a $\underline{24}$ or $\underline{75}$, and correspondingly transform. Since our textures are to a large extent a minimal extension of the GJ ones,

⁴But clearly, flavour models do depend on the choice of basis since their symmetries do not commute with basis transformations.

their well known mechanism can be simply incorporated; the fit of the quark mass matrices of Section 5 then leads to lepton masses that agree with experimental values to $O(10\%)$, the largest deviation concerning $b-\tau$ unification [21]. At difference of the quark sector, we do not attempt a better fit for lepton masses as it would drastically depend on the details of the supersymmetric model [22] and, possibly, on threshold effects due to heavy particles [23]. Since lepton mixings are less sensitive to these details, they can be qualitatively analysed by using the lepton textures obtained with the simple GJ prescription: while the first set displays small mixings for both chiralities, the second set has a maximal $\mu-\tau$ mixing for the left-handed charged leptons.

2 Conventions and Preliminaries

In the basis of the unknown flavour symmetry the Lagrangian is described by

$$\begin{aligned} \mathcal{L} = & - \bar{u}_R^T \mathbf{m}_u u_L - \bar{d}_R^T \mathbf{m}_d d_L - \frac{1}{2} \nu^T \mathbf{m}_\nu^{eff} \nu - \bar{e}_R^T \mathbf{m}_e e_L \\ & + \frac{g}{\sqrt{2}} \bar{u}_L^T \gamma^\lambda d_L W_\lambda^+ + \frac{g}{\sqrt{2}} \bar{e}_L^T \gamma^\lambda \nu W_\lambda^- + \text{h.c.} \end{aligned} \quad (1)$$

$$\mathbf{m}_u = U_{u_R} \hat{m}_u U_{u_L}^\dagger \quad , \quad \mathbf{m}_d = U_{d_R} \hat{m}_d U_{d_L}^\dagger \quad , \quad \mathbf{m}_\nu^{eff} = U_\nu^* \hat{m}_\nu U_\nu^\dagger \quad , \quad \mathbf{m}_e = U_{e_R} \hat{m}_e U_{e_L}^\dagger \quad (2)$$

where a hat is placed over a diagonal matrix with real positive eigenvalues whose order is established conventionally by requiring $|m_2^2 - m_3^2| \geq m_2^2 - m_1^2 \geq 0$, and the U 's are unitary matrices. The CKM and MNS mixing matrices are respectively

$$V_{CKM} = U_{u_L}^\dagger U_{d_L} \quad , \quad U_{MNS} = U_{e_L}^\dagger U_\nu \quad . \quad (3)$$

Diagonalization proceeds, at left and right, alternating rotations and phase transformations. In particular, we introduce

$$\begin{aligned} R_{23}(\theta_{23}) &= \begin{pmatrix} 1 & 0 & 0 \\ 0 & c_{23} & s_{23} \\ 0 & -s_{23} & c_{23} \end{pmatrix}, \quad R_{13}(\theta_{13}) = \begin{pmatrix} c_{13} & 0 & s_{13} \\ 0 & 1 & 0 \\ -s_{13} & 0 & c_{13} \end{pmatrix}, \quad R_{12}(\theta_{12}) = \begin{pmatrix} c_{12} & s_{12} & 0 \\ -s_{12} & c_{12} & 0 \\ 0 & 0 & 1 \end{pmatrix}, \\ \Phi &= \text{diag}(\phi_{12} + \phi_{23}, \phi_{23}, 1) \quad , \quad \Phi' = \text{diag}(\phi'_1, \phi'_2, \phi'_3) \quad , \end{aligned} \quad (4)$$

where $s_{ij} = \sin \theta_{ij}$, $c_{ij} = \cos \theta_{ij}$. We find particularly convenient to parameterize each U appearing in eq. (2), as well as V_{CKM} and U_{MNS} themselves, in terms of a matrix in the standard CKM parameterization $U^{(s)}$ [17], multiplied at left and right by diagonal matrices of phases of the form of Φ and Φ' . Leaving indices understood,

$$U = e^{i\Phi} U^{(s)} e^{i\Phi'} \quad , \quad U^{(s)} = R_{23}(\theta_{23}) \Gamma_\delta R_{13}(\theta_{13}) \Gamma_\delta^\dagger R_{12}(\theta_{12}) \quad (5)$$

where $\Gamma_\delta = \text{diag}(1, 1, e^{i\delta})$, angles belong to $[0, \pi/2]$ and phases to $]-\pi, \pi]$.

The phases Φ' of charged fermions can be removed by means of unitary transformations acting on right-handed fields. Defining $\Phi_q = \Phi_{u_L} - \Phi_{d_L}$, $\Phi_\ell = \Phi_{e_L} - \Phi_\nu$, one then obtains⁵

$$V_{CKM} = U_{u_L}^{(s)\dagger} e^{-i\Phi_q} U_{d_L}^{(s)} \quad , \quad U_{MNS} = U_{e_L}^{(s)\dagger} e^{-i\Phi_\ell} U_\nu^{(s)} e^{i\Phi'_\nu} \quad . \quad (6)$$

The phases $\phi_{ij}^q = \phi_{ij}^{u_L} - \phi_{ij}^{d_L}$ and $\phi_{ij}^\ell = \phi_{ij}^{e_L} - \phi_{ij}^\nu$ ($ij = 12, 23$) can be chosen in $]-\pi, \pi]$ and represent the phase difference between the i -th and the $i+1$ -th generation of left-handed quarks and leptons respectively, before shuffling the flavors to go in the mass basis. They cannot be removed and, although not individually measurable⁶, are a source for CP violation and play a crucial role in the mixing matrices - see e.g. [5, 7, 12, 16]. Note that low energy CPV in the CKM (MNS) matrix can be generated in the limit where only $\phi_{12}^{q(\ell)}$ and/or $\phi_{23}^{q(\ell)}$ are present, as well as in the limit where there are just $\delta^{u_L(e_L)}$ and/or $\delta^{d_L(\nu)}$.

In a grand unified theory like $SU(5)$, one expects $m_e \approx m_d^T$, where the coefficients may be different for the elements coming from a (fundamental or effective) $\overline{45}$ Higgs representation. From $U_{e_L} \approx U_{d_R}^*$, it follows that $\Phi_{e_L} \approx -\Phi_{d_R}$. The CPV phases of Φ_{d_R} , irrelevant for the quark sector, are thus important for the lepton sector, as they explicitly appear in the expression for U_{MNS} . In such a framework, it is interesting to investigate possible connections between CPV in quarks and leptons, as will be done in Section 6.

3 Guidelines of the Approach

The goal of the subsequent approach, based on a couple of assumptions, is to establish possible relations among ratios of quark masses, angles and phases of V_{CKM} , at the low energy scale m_Z . This discussion turns out to provide useful guidelines to be exploited in Section 4, where a more general analysis will be provided. Clearly, some observations are already present in the literature, though obtained with different approaches. We update and combine them from a point of view that allows to cleanly identify the weak points and to introduce our proposed solutions.

Firstly, it is well known that the phenomenological relation $|V_{ub}| = O(|V_{us}V_{cb}|)$ supports the possibility that $\theta_{13}^{u_L}$ and $\theta_{13}^{d_L}$ are small enough to negligibly contribute to $|V_{ub}|$. Also the associated phases δ^{u_L} and δ^{d_L} become irrelevant, so that the fundamental CKM parameters appearing in the r.h.s. eq. (6) are reduced from ten to six: four near-neighbor generation mixing angles and the two phases of Φ_q ⁷. Then, a non-vanishing $|V_{ub}|$ arises

⁵ Φ'_ν solely contributes to Majorana CPV phases.

⁶Of course, none of the 10 (12) parameters appearing in the r.h.s. of eqs. (6) is measurable.

⁷Still, there is redundancy with respect to measurable quantities but, at difference of previous analysis [5, 7, 8], we prefer to carry out the discussion explicitly in terms of these six parameters in order to see separately the role played by ϕ_{12}^q and ϕ_{23}^q in the CKM matrix.

in V_{CKM} as the result of re-arranging $R_{12}^{u_L T}$ at the right of $R_{23}^{u_L T} R_{23}^{d_L}$. Explicitly, from eq. (6) one gets:

$$|V_{ub}| = s_{12}^{u_L} |s_{23}^{d_L} c_{23}^{u_L} e^{-i\phi_{23}^q} - s_{23}^{u_L} c_{23}^{d_L}| = \frac{s_{12}^{u_L}}{s_{12}^{d_L}} |V_{td}| \quad , \quad (7)$$

$$|V_{cb}| = \frac{c_{12}^{u_L}}{s_{12}^{u_L}} |V_{ub}| \quad , \quad |V_{ts}| = \frac{c_{12}^{d_L}}{s_{12}^{d_L}} |V_{td}| \quad , \quad (8)$$

$$|V_{us}| = |s_{12}^{d_L} c_{12}^{u_L} e^{-i\phi_{12}^q} - c_{23}^{u_L} s_{12}^{u_L} c_{23}^{d_L} c_{12}^{d_L} - s_{23}^{u_L} s_{12}^{u_L} s_{23}^{d_L} c_{12}^{d_L} e^{i\phi_{23}^q}| \quad . \quad (9)$$

Analogous expressions hold for the corresponding elements of U_{MNS} if one attributes the smallness of $|U_{e3}|$ to the individual smallness of $\theta_{13}^{e_L}$ and θ_{13}^ν . In such a case, due to $|U_{\mu 3}| \approx 1/\sqrt{2}$, one also has $s_{12}^{e_L} \lesssim |U_{e3}|$.

Secondly, the smallness of the CKM mixing angles suggests that, to avoid large cancellations between U_{u_L} and U_{d_L} , their mixings should be individually small. In the $c_{12}^{u_L} = c_{12}^{e_L} = 1$ approximations, one obtains the two formally similar expressions:

$$|V_{cb}| \simeq |s_{23}^{d_L} c_{23}^{u_L} - e^{-i\phi_{23}^q} s_{23}^{u_L} c_{23}^{d_L}| \quad , \quad |U_{\mu 3}| \simeq |s_{23}^\nu c_{23}^{e_L} - e^{-i\phi_{23}^\ell} s_{23}^{e_L} c_{23}^\nu| \quad . \quad (10)$$

Since the experimental range in the l.h.s. is different, different regions in the domains $\{s_{23}^{u_L}, s_{23}^{d_L}, \phi_{23}^q\}$ and $\{s_{23}^\nu, s_{23}^{e_L}, \phi_{23}^\ell\}$ are allowed, as displayed in fig. 2 for $\phi_{23}^{q,\ell} = 0, \pm\pi/4, \pm\pi/2, \pi$. On the quark side, $s_{23}^{u_L}$ and $s_{23}^{d_L}$ have to be small in order to avoid tunings, as just mentioned. Notice that the identifications $s_{23}^{u_L} = \sqrt{m_c/m_t}$ and $s_{23}^{d_L} = m_s/m_b$, corresponding to the shaded rectangular region, suggest $\phi_{23}^q \approx 0$. On the lepton side, the possibility $\phi_{23}^\ell = \pm\pi/2$ turns out to be very attractive: if $\theta_{23}^{e_L} = \pi/4$, a maximal atmospheric angle is obtained for whatever value of θ_{23}^ν , and viceversa.

Neglecting terms of second order in $s_{23}^{u_L}$ and $s_{23}^{d_L}$, the expressions for $|V_{us}|$ and the angles of the unitarity triangle become easy to handle⁸:

$$e^{i\beta} |V_{us}| \simeq s_{12}^{d_L} c_{12}^{u_L} - e^{-i\phi_{12}^q} s_{12}^{u_L} c_{12}^{d_L} \quad , \quad \alpha \simeq \phi_{12}^q - \arg(1 + e^{i\phi_{12}^q} \frac{s_{12}^{u_L} s_{12}^{d_L}}{c_{12}^{u_L} c_{12}^{d_L}}) \quad . \quad (11)$$

It turns out that *the sole source of CP violation in V_{CKM} is ϕ_{12}^q* , as a dependence on ϕ_{23}^q in eq. (11) would be introduced by negligible terms proportional to $s_{23}^{u_L} s_{23}^{d_L}$. The above expression for $|V_{us}|$, formally similar to those in eq. (10), selects appropriate regions in the domain $\{s_{12}^{u_L}, s_{12}^{d_L}, \phi_{12}^q\}$, as displayed in fig. 3 for $\phi_{12}^q = 0, \pm\pi/4, \pm\pi/2, \pi$. In particular, for $\phi_{12}^q = \pm\pi/2$ the circumference of radius $|V_{us}|$ in the plane $\{s_{12}^{u_L}, s_{12}^{d_L}\}$ is selected, which nicely overlaps the broader rectangular region consistent with the identifications

⁸We do not write the analogous expressions for the lepton sector as the large atmospheric mixing prevent us from taking small $s_{23}^{e_L}$ and s_{23}^ν .

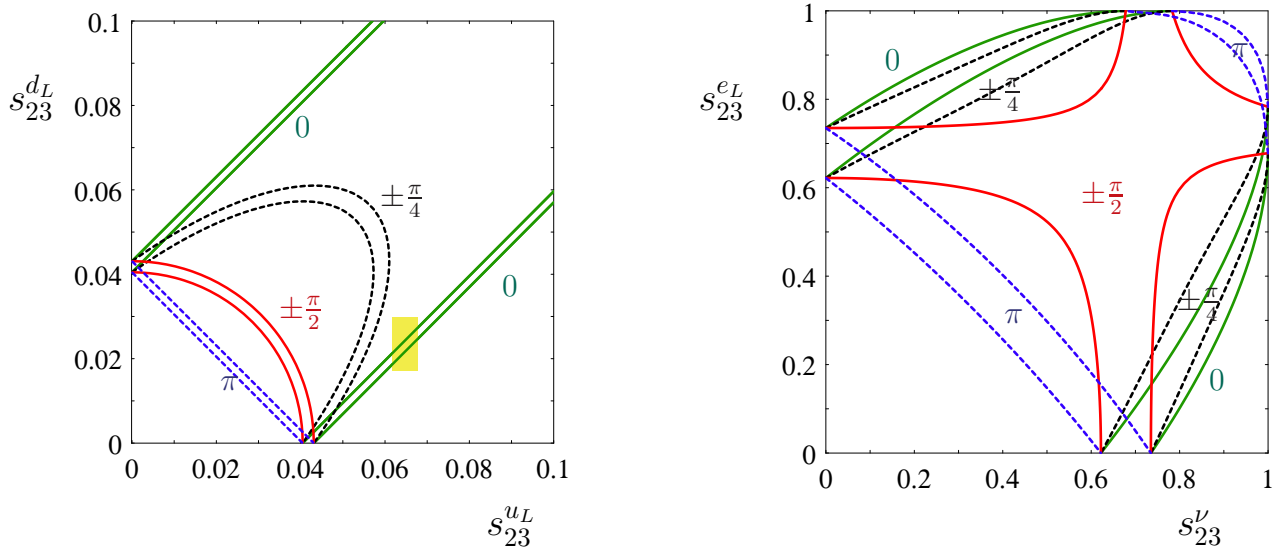


Figure 2: Left: stripes consistent with $|\mathcal{V}_{cb}|$ at 2σ [14] in the plane $\{s_{23}^{u_L}, s_{23}^{d_L}\}$ for $\phi_{23}^q = 0, \pm\pi/4, \pm\pi/2, \pi$. The shaded rectangular region corresponds to the identifications $s_{23}^{u_L} = \sqrt{m_c/m_t}$ and $s_{23}^{d_L} = m_s/m_b$ at m_Z , according to the PDG mass estimates [17]. Right: stripes consistent with $|\mathcal{U}_{\mu 3}|$ at 1σ [24] in the plane $\{s_{23}^{\nu}, s_{23}^{e_L}\}$ for $\phi_{23}^{\ell} = 0, \pm\pi/4, \pm\pi/2, \pi$.

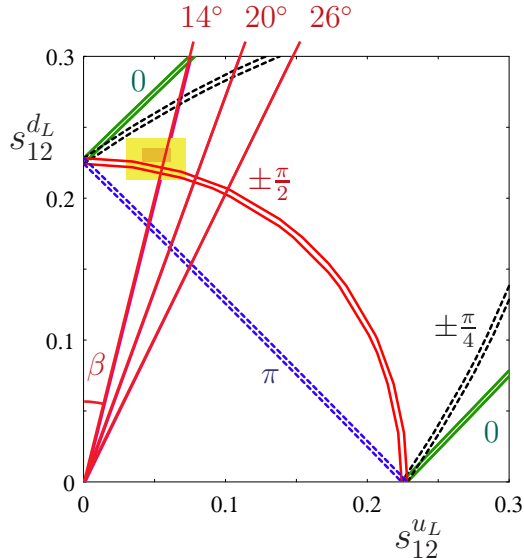


Figure 3: Stripes consistent with $|\mathcal{V}_{us}|$ at 2σ [14] in the plane $\{s_{12}^{u_L}, s_{12}^{d_L}\}$ for $\phi_{12}^q = 0, \pm\pi/4, \pm\pi/2, \pi$. The larger (yellow) and smaller (orange) shaded rectangular regions correspond to the identifications $s_{12}^{u_L} = \sqrt{m_u/m_c}$, $s_{12}^{d_L} = \sqrt{m_d/m_s}$ at m_Z , respectively according to the PDG [17] and to the CPT mass estimates [19]. For $\phi_{12}^q = +\pi/2$, the straight lines show the value assumed by β - see eq. (12).

$s_{12}^{u_L} = \sqrt{m_u/m_c}$, $s_{12}^{d_L} = \sqrt{m_d/m_s}$, as given by the PDG [17]. The overlap would be poor considering instead the smaller rectangular region consistent with CPT analysis [19].

Also the fact that the unitarity triangle is at present compatible with rectangle suggests the remarkable value $\phi_{12}^q = +\pi/2$, in agreement with the above discussion on $|V_{us}|$ but solving in addition the sign ambiguity. Taking $\phi_{12}^q = \pi/2$ and neglecting terms of second order in $s_{12}^{u_L}$ and $s_{12}^{d_L}$, one has simply⁹

$$\alpha \simeq \frac{\pi}{2} \quad , \quad \tan \beta \simeq \frac{s_{12}^{u_L}}{s_{12}^{d_L}} \quad . \quad (12)$$

As shown in fig. 3, the identifications $s_{12}^{u_L} = \sqrt{m_u/m_c}$ and $s_{12}^{d_L} = \sqrt{m_d/m_s}$ would point towards relatively small values of β , as compared to the present 1σ average of BaBar and Belle: $\beta = 21.7^{+1.3}_{-1.2}^\circ$ [13]. Since from eq. (8) $s_{12}^{u_L} \simeq |V_{ub}/V_{cb}|$ and $s_{12}^{d_L} \simeq |V_{td}/V_{ts}|$, these identifications would also point towards respectively low and large values of $|V_{ub}/V_{cb}|$ and $|V_{td}/V_{ts}|$, whose 2σ ranges are $0.087 - 0.099$ and $0.173 - 0.224$ according to [14].

A compromise is reached for small m_d/m_s and large m_u/m_c : e.g. $\sqrt{m_d/m_s} = 0.22$, $\sqrt{m_u/m_c} = 0.08$, in which case $\beta = 20^\circ$. However, a more accurate analysis reveals a problem: since $m_c/m_s \geq 8$ at m_Z , one has $m_u/m_d \geq 1$, in rough contrast with the PDG interval $m_u/m_d = 0.5 \pm 0.2$ [17] and, a fortiori, with the CPT prediction, $m_u/m_d = 0.553 \pm 0.043$ [19]. In summary, a better fit to β and $|V_{ub}/V_{cb}|$ would require a value of m_u/m_d (or equivalently, m_u/m_c) which is about three times as much as the CPT estimate.

3.1 Textures for a First Approximation

Given the delicate problem of the definition of light quark masses, it is nevertheless suggestive that the experimental data allow for such a simple interpretation in terms of angles being related to the mentioned ratios of masses and CPV stemming just from $\phi_{12}^q = \pi/2 \simeq \alpha$. A pair of textures with all such characteristics is¹⁰:

$$\mathbf{m}_u = \begin{pmatrix} 0 & \sqrt{\frac{m_u m_c}{m_t^2}} & 0 \\ \sqrt{\frac{m_u m_c}{m_t^2}} & 0 & \sqrt{\frac{m_c}{m_t}} \\ 0 & \sqrt{\frac{m_c}{m_t}} & 1 \end{pmatrix} y_t \frac{v_u}{\sqrt{2}} \quad , \quad \mathbf{m}_d = \begin{pmatrix} 0 & \sqrt{\frac{m_d m_s}{m_b^2}} & 0 \\ \sqrt{\frac{m_d m_s}{m_b^2}} & i \frac{m_s}{m_b} & 0 \\ 0 & \frac{m_s}{m_b} & 1 \end{pmatrix} y_b \frac{v_d}{\sqrt{2}} \quad . \quad (14)$$

⁹Notice that $\pi/2$ is close to the value of ϕ_{12}^q that maximizes β .

¹⁰As we are going to discuss in the next section, \mathbf{m}_d could be equivalently replaced by

$$\mathbf{m}_d = \begin{pmatrix} 0 & \sqrt{\frac{m_d m_s}{m_b^2}} & 0 \\ \frac{1}{\sqrt{2}} \sqrt{\frac{m_d m_s}{m_b^2}} & i \sqrt{2} \frac{m_s}{m_b} & \frac{i}{\sqrt{2}} \\ \frac{i}{\sqrt{2}} \sqrt{\frac{m_d m_s}{m_b^2}} & 0 & \frac{1}{\sqrt{2}} \end{pmatrix} y_b \frac{v_d}{\sqrt{2}} \quad . \quad (13)$$

There are two small parameters in each texture, that induce only near-neighbor mixings and determine the mass ratios in the corresponding sector. The unique maximal source of CP violation is the purely imaginary 22-element of \mathbf{m}_d , which leads to

$$\alpha \approx \frac{\pi}{2} \quad , \quad \tan \beta \approx \sqrt{\frac{m_u m_s}{m_d m_c}} \quad . \quad (15)$$

In summary, 8 observable quantities (1 phase, 3 angles, 4 mass ratios) uncorrelated in the SM are not badly reproduced in terms of textures having 4 parameters and real elements, but for a purely imaginary one. As far as we know, these particular textures have not been emphasized previously. Notice that they are a renewed version of the GJ ones (where $\mathbf{m}_{d32} = 0$ and it was premature to address the issue of CPV), with the imaginary element being the Yukawa coupling associated to the $SU(5)$ -breaking v.e.v. responsible for the difference in the spectrum of down-quarks and charged leptons (more on this later).

Since taking $\mathbf{m}_{d23} = m_s/m_b$ in eq. (14) has negligible impact on the previous discussion, in practice these textures belong to the category of hierarchical symmetric textures with zeros in the 11,13,31 elements, studied in detail in refs. [5, 9, 11]. There, it was shown that their general predictions [5] $|V_{ub}/V_{cb}| \approx \sqrt{m_u/m_c}$ and $\tan \beta \lesssim \sqrt{m_u m_s/m_c m_d}$ are barely compatible with experiment - see respectively ref. [9] and [11]. Even though data have changed in the meantime (in particular β is now slightly smaller, as can be seen in fig. 1) these conclusions remain valid.

It is worth to signal immediately a possible remedy, which we are going to exploit in the following section. We already discussed that by taking $s_{12}^{u_L} \approx \sqrt{3m_u/m_c}$ while keeping the other identifications of angles with mass ratios, one properly enhances β and $|V_{ub}/V_{cb}|$ without affecting $\alpha \simeq \pi/2$. This factor of 3 could be induced through a slight modification of \mathbf{m}_u , namely by filling the zero in the 11-element with a parameter smaller than those already introduced.

3.2 On the Effect of $\theta_{13}^{u_L, d_L} \neq 0$

It could seem that $s_{13}^{u_L} \neq 0$ and/or $s_{13}^{d_L} \neq 0$ help in solving the problem with β and $|V_{ub}/V_{cb}|$. Instead we show here that the present data on α disfavor this possibility. For the textures in eq. (14), this modification would be realized e.g. by filling the zero in \mathbf{m}_{u31} and/or \mathbf{m}_{d31} , but we prefer to discuss the argument from a more general point of view.

Assuming that left-chirality quark mixings are small, the expression for $|V_{us}|$ in eq. (11) is practically unaffected, and so is $|V_{cb}|$ in eq. (10) if $s_{13}^{d_L}, s_{13}^{u_L} \ll |V_{cb}|/s_{12}^{u_L}$. On the contrary, defining

$$e^{i\phi_{cb}}|V_{cb}| \simeq -s_{23}^{d_L} c_{23}^{u_L} e^{-i\phi_{23}^q} + s_{23}^{u_L} c_{23}^{d_L} \quad , \quad e^{i\phi_{us}}|V_{us}| \simeq s_{12}^{d_L} c_{12}^{u_L} - e^{-i\phi_{12}^q} s_{12}^{u_L} c_{12}^{d_L} \quad , \quad (16)$$

and neglecting for simplicity the terms of second order in $s_{12}^{u_L}$ and $s_{12}^{d_L}$:

$$\begin{aligned} e^{-i\xi_b} \left| \frac{V_{ub}}{V_{cb}} \right| &\simeq \frac{s_{12}^{u_L}}{c_{12}^{u_L}} + \frac{s_{13}^{d_L}}{|V_{cb}|} e^{i(\delta^{d_L} + \phi_{12}^q + \phi_{23}^q + \phi_{cb})} - \frac{s_{13}^{u_L}}{|V_{cb}|} e^{i(\delta^{u_L} + \phi_{cb})} \quad , \\ e^{-i\xi_t} \left| \frac{V_{td}}{V_{ts}} \right| &\simeq \frac{s_{12}^{d_L}}{c_{12}^{d_L}} + \frac{s_{13}^{d_L}}{|V_{cb}|} e^{i(\delta^{d_L} + \phi_{23}^q + \phi_{cb})} - \frac{s_{13}^{u_L}}{|V_{cb}|} e^{i(\delta^{u_L} - \phi_{12}^q + \phi_{cb})} \quad , \\ \alpha &\simeq \phi_{12}^q - \xi_t + \xi_b \quad , \quad \beta \simeq \phi_{us} + \xi_t \quad . \end{aligned} \quad (17)$$

For $s_{13}^{d_L(u_L)}$ to be effective in correcting $|V_{ub}/V_{cb}|$, one needs $s_{13}^{d_L(u_L)} \approx s_{12}^{u_L} |V_{cb}|$, in agreement with the hypothesis that $|V_{cb}|$ is slightly affected.

We now take $\phi_{12}^q = \pi/2$, $\phi_{23}^q = 0$ (hence $\phi_{cb} = 0$) and consider the effect of $s_{13}^{d_L(u_L)}$ only. As one can see from eqs. (17), $|V_{ub}/V_{cb}|$ is maximized for $\delta^{d_L} = -\pi/2$ ($\delta^{u_L} = \pi$) while, at the same time, $|V_{td}/V_{ts}|$ is negligibly affected, ξ_b vanishes, $\tan \xi_t = \frac{c_{12}^{d_L}}{s_{12}^{d_L} |V_{cb}|} s_{13}^{d_L(u_L)}$ and

$$\alpha \simeq \frac{\pi}{2} - \xi_t \quad , \quad \beta \simeq \arctan\left(\frac{s_{12}^{u_L}}{s_{12}^{d_L}}\right) + \xi_t \quad . \quad (18)$$

With respect to their values in eq. (12), β and α are respectively enhanced and lowered by ξ_t . Fig. 3 shows that, in order to fit β and $|V_{ub}/V_{cb}|$ while keeping the identifications $s_{12}^{u_L} = \sqrt{m_u/m_c}$ and $s_{12}^{d_L} = \sqrt{m_d/m_s}$, one needs $\xi_t \sim 8^\circ$. However, *all this happens at the price of turning α down to 82° , close to its 2σ lower range*.

This remedy was implemented for hierarchical symmetric textures with zeros in the 11,13,31 elements in order to properly enhance their predictions for β and $|V_{ub}/V_{cb}|$, in particular by filling \mathbf{m}_{d31} [9, 11]. Also for hermitian mass matrices with vanishing 11-elements, the importance of the so-called "non-factorizable" phase δ^{d_L} to possibly enhance β was pointed out [12]. However, the correlation between α and β did not emerge as the constraint on α were much weaker at that time. The present inadequacy of this remedy¹¹ prompted us in re-addressing the issue of finding simple textures that correctly reproduce the data.

As already mentioned, for the purpose of enhancing β and $|V_{ub}/V_{cb}|$ a better remedy that we are going to adopt in the next section consists in filling the zero of \mathbf{m}_{u11} to obtain $s_{12}^{u_L} \approx \sqrt{3m_u/m_c}$. In top of this, one could successfully exploit a non vanishing $s_{13}^{d_L(u_L)}$ but with $\delta^{d_L} = \pi$ ($\delta^{u_L} = \pi/2$). Indeed, in this case $\xi_t = 0$, $\tan \xi_b = \frac{c_{12}^{u_L}}{s_{12}^{u_L} |V_{cb}|} s_{13}^{d_L(u_L)}$ and

$$\alpha \simeq \frac{\pi}{2} + \xi_b \quad , \quad \beta \simeq \arctan\left(\frac{s_{12}^{u_L}}{s_{12}^{d_L}}\right) \quad . \quad (19)$$

¹¹Actually, for some values of $s_{13}^{d_L}$ one can find corresponding values of δ^{d_L} that give a good fit to both α and β . Such values of δ^{d_L} being not close to zero or $\pi/2$, this amounts to introducing one more parameter in the texture. We thank A. Romanino for calling our attention to this possibility.

Having $\xi_b \sim 8^\circ$ makes α reach its present central value, about 98° , without affecting β . Depending on the closeness of α to $\pi/2$, future experiments will clarify whether such further correction is really needed. Notice also that, in this case, $|V_{td}/V_{ts}|$ gets lowered while $|V_{ub}/V_{cb}|$ is negligibly affected.

4 The Textures for \mathbf{m}_u and \mathbf{m}_d

We now proceed to determine textures defined at m_Z in good agreement with experiment and fulfilling the conditions identified in the previous section. The Wolfenstein parameterization of the CKM matrix [25] in terms of powers of $\lambda = \sin \theta_C$ suggests to do the same for the mass matrices. We assume that the textures $\mathbf{T}_u = \frac{\sqrt{2}\mathbf{m}_u}{y_t v_u}$ and $\mathbf{T}_d = \frac{\sqrt{2}\mathbf{m}_d}{y_b v_d}$ are

$$\mathbf{T}_u = \begin{pmatrix} e^{i\phi_c} c \lambda^8 & a\lambda^6 & 0 \\ a\lambda^6 & 0 & b\lambda^2 \\ 0 & b\lambda^2 & 1 \end{pmatrix} \quad , \quad \mathbf{T}_d = \begin{pmatrix} < O(\lambda^5) & g \lambda^3 & e^{i\phi_n} n \lambda^3 \\ g' \lambda^3 & e^{i\phi_j} j \lambda^2 & e^{i\phi_t} t \\ e^{i\phi_m} m \lambda^3 & e^{i\phi_k} k \lambda^2 & 1 \end{pmatrix} \frac{1}{\sqrt{1+t^2}} \quad , \quad (20)$$

where $\lambda = 0.23$, $a, b, c, g, g', j, t, m, n, k$ are $O(1)$ real positive numbers, some non-physical phases have already been removed and the remaining ones are chosen for definiteness in $]-\pi, \pi]$.

For up quarks, introducing $r_u = |1 + e^{i\phi_c} \frac{cb^2}{a^2}|$, one has at leading order

$$\sqrt{\frac{m_u}{m_c}} \simeq \sqrt{r_u} \frac{a}{b^2} \lambda^2 \quad , \quad \sqrt{\frac{m_c}{m_t}} \simeq b\lambda^2 \quad , \quad (21)$$

$$s_{23}^{u_L, u_R} \simeq \sqrt{\frac{m_c}{m_t}} \quad , \quad s_{13}^{u_L, u_R} \simeq O(\lambda^8) \quad , \quad s_{12}^{u_L, u_R} \simeq \sqrt{\frac{1}{r_u} \frac{m_u}{m_c}} \quad , \quad (22)$$

$$\phi_{12}^{u_L, u_R} = \pi \quad , \quad \phi_{23}^{u_L, u_R} = 0 \quad . \quad (23)$$

For down quarks, introducing $r_d = \frac{|g' - e^{i(\phi_m + \phi_t)} mt|}{g\sqrt{1+t^2}}$, one has at leading order

$$e^{-i\phi_{12}^{d_L}} \sqrt{\frac{m_d}{m_s + m_d}} \simeq \frac{1}{\sqrt{r_d}} \frac{g' - e^{i(\phi_m + \phi_t)} mt}{e^{i\phi_j} j - e^{i(\phi_t + \phi_k)} tk} \lambda \quad , \quad e^{-i\phi_{12}^{d_R}} \frac{m_s}{m_b} \simeq \frac{e^{i\phi_j} j - e^{i(\phi_t + \phi_k)} tk}{1 + t^2} \lambda^2 \quad , \quad (24)$$

$$s_{23}^{d_L} e^{-i\phi_{23}^{d_L}} \simeq \frac{e^{i(\phi_j - \phi_t)} tj + e^{i\phi_k} k}{1 + t^2} \lambda^2 \quad , \quad s_{23}^{d_R} e^{-i\phi_{23}^{d_R}} \simeq e^{-i\phi_t} \frac{t}{\sqrt{1+t^2}} \quad , \quad (25)$$

$$s_{13}^{d_L} e^{i\phi_{13}^{d_L}} \simeq e^{-i\phi_t} \frac{tg' + e^{i(\phi_m + \phi_t)} m}{1 + t^2} \lambda^3 \quad , \quad s_{13}^{d_R} e^{i\phi_{13}^{d_R}} \simeq e^{-i\phi_n} \frac{n}{\sqrt{1+t^2}} \lambda^3 \quad , \quad (26)$$

$$s_{12}^{d_L} \simeq \sqrt{r_d \frac{m_d}{m_s + m_d}} \quad , \quad s_{12}^{d_R} \simeq \sqrt{\frac{1}{r_d} \frac{m_d}{m_s + m_d}} \quad . \quad (27)$$

In particular, as for the phases one ends up with

$$\phi_{23}^q = -\phi_{23}^{d_L} \quad , \quad \phi_{12}^q = \pi - \phi_{12}^{d_L} \quad , \quad \delta^{d_L} = \delta_{13}^{d_L} - \phi_{23}^q - \phi_{12}^q + \pi \quad . \quad (28)$$

Because the mixing angles are often better known than the masses, we now express the CKM elements as a function of the quark mass ratios. We already know from the previous discussion that, having $s_{23}^{u_L} \simeq \sqrt{m_c/m_t}$, it is desirable to also have $s_{23}^{d_L} \simeq m_s/m_b$. From eq. (25), one realizes that this can be achieved naturally in three cases, which correspond to put a zero respectively in the 23,32,22 element of \mathbf{T}_d : 1) $t = 0, k = j$; 2) $t = 1, k = 0$; 3) $t = 1, j = 0$. Since $\lambda^3 \sim s_{13}^{d_L} \ll |V_{cb}|/s_{12}^{u_L} \sim 1$, in all these cases

$$|V_{cb}| \simeq \left| \sqrt{\frac{m_c}{m_t}} - e^{-i\phi_{23}^q} \frac{m_s}{m_b} \right| \quad (29)$$

and, as can be seen from fig. 4, small values of ϕ_{23}^q are favored. According to the various cases, the condition $\phi_{23}^q = 0$ reads: 1) $\phi_k = 0$; 2) $\phi_j = \phi_t$; 3) $\phi_k = 0$.

Having $s_{12}^{u_L} = O(\sqrt{m_u/m_c})$, we also know that it would be convenient to enforce $s_{12}^{d_L} = \sqrt{m_d/m_s}$, namely $r_d = 1$, which is realized in the various cases for: 1) $g' = g$; 2)&3) $g\sqrt{2} = g_{||}$, where $e^{i\gamma_{||}} g_{||} = g' - e^{i(\phi_m + \phi_t)} m$. In all these cases then

$$|V_{us}| \simeq \sqrt{\frac{m_s}{m_d + m_s}} \left| \sqrt{\frac{m_d}{m_s}} - e^{-i\phi_{12}^q} \sqrt{\frac{1}{r_u} \frac{m_u}{m_c}} \right| \quad (30)$$

and, as can be seen from fig. 4, the experimental value of $|V_{us}|$ favors ϕ_{12}^q close to $\pm\frac{\pi}{2}$. For the three cases, this would imply: 1) $\phi_j \approx \pm\frac{\pi}{2}$; 2) $\phi_j \approx \pm\frac{\pi}{2} + \gamma_{||}$; 3) $\phi_k \approx \mp\frac{\pi}{2} + \gamma_{||}$.

Using these results, we now turn to consider the effect of $s_{13}^{d_L}$. By adapting eq. (26) one has: 1) $s_{13}^{d_L} \simeq \frac{m}{g} \frac{m_s}{m_b} \sqrt{\frac{m_d}{m_s}}$; 2)&3) $s_{13}^{d_L} \simeq \frac{g_{\perp}}{g_{||}} \frac{m_s}{m_b} \sqrt{\frac{m_d}{m_s}}$, where $g_{\perp} = |g' + e^{i(\phi_m + \phi_t)} m|$. In particular, it turns out that the requirement $s_{13}^{d_L} = 0$ is fulfilled when: 1) $m = 0$; 2)&3) $g_{\perp} = 0$, i.e. $\phi_t + \phi_m = \pi$ and $g' = m$, so that also $\gamma_{||} = 0$. Then, following the discussion in the previous section, one finds the simple relations

$$\begin{aligned} \left| \frac{V_{ub}}{V_{cb}} \right|^2 &\simeq \frac{1}{r_u} \frac{m_u}{m_c} \quad , & \left| \frac{V_{td}}{V_{ts}} \right|^2 &\simeq \frac{m_d}{m_s} \quad , \\ \alpha \simeq \phi_{12}^q &\quad , & \beta \simeq \arg \left(\sqrt{\frac{m_d}{m_s}} - e^{-i\phi_{12}^q} \sqrt{\frac{1}{r_u} \frac{m_u}{m_c}} \right) &\quad . \end{aligned} \quad (31)$$

As can be checked from fig. 4, to satisfy all these constraints it is better to have $\phi_{12}^q = +\frac{\pi}{2}$. The CPT estimate then suggests $r_u \approx 1/3$. This is realized for instance with $\phi_c = \pi$ and $cb^2/a^2 \approx 2/3$ or $4/3$. Notice that, for the various cases, the condition $\phi_{12}^q = +\frac{\pi}{2}$ reads:

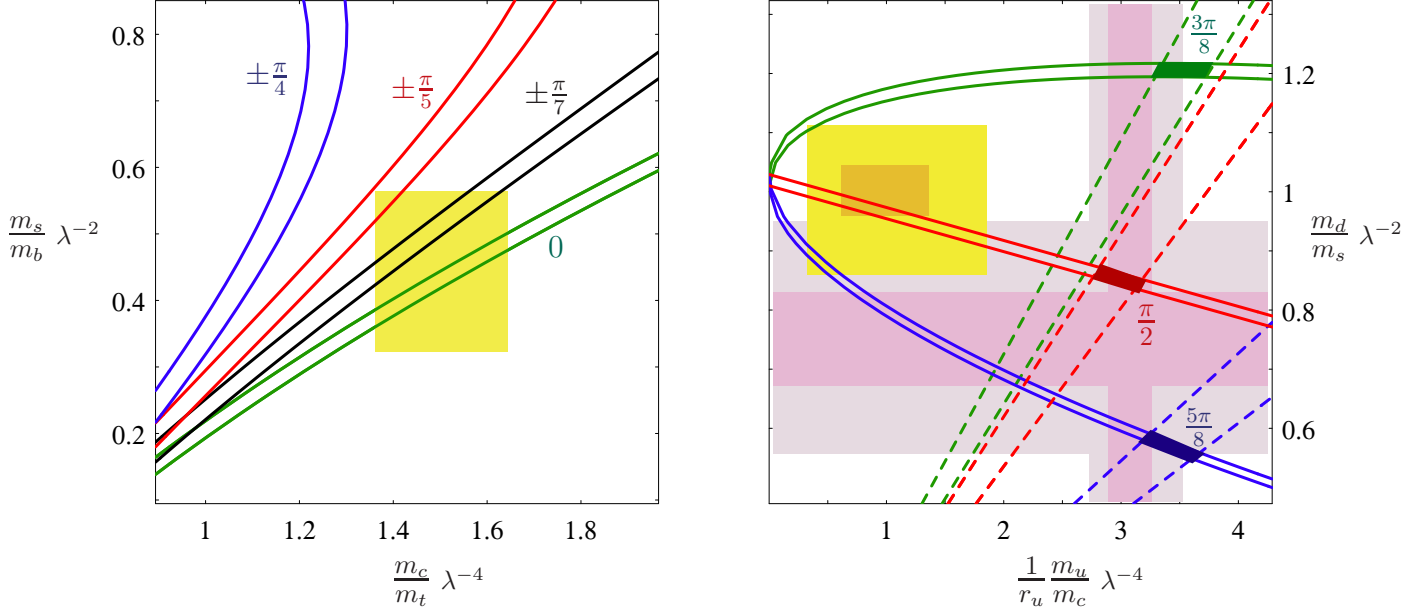


Figure 4: Left: stripes consistent with $|V_{cb}|$ at 1σ [14] for $\phi_{23}^q = 0, \pm\pi/7, \pm\pi/5, \pm\pi/4$. The shaded rectangle is the range for the mass ratios according to PDG [17]. Right: stripes consistent with $|V_{us}|$ (full) and β (dashed) at 1σ for $\phi_{12}^q = 5\pi/8, \pi/2, 3\pi/8$, with intersections emphasized. The shaded vertical and horizontal bands signal the values of $|V_{ub}/V_{cb}|$ and $|V_{td}/V_{ts}|$ at $1,2\sigma$. The larger and smaller shaded rectangles display the range of the mass ratios ($r_u = 1$) according to PDG [17] and CPT estimates [19] respectively.

1)&2) $\phi_j = \frac{\pi}{2}$; 3) $\phi_k = -\frac{\pi}{2}$, in conflict with the former condition $\phi_{23}^q = \phi_k = 0$. In the following we then abandon case 3).

Summarizing the results, the data suggest the simple structures¹²

$$\mathbf{T}_u = \begin{pmatrix} -c\lambda^8 & a\lambda^6 & 0 \\ a\lambda^6 & 0 & b\lambda^2 \\ 0 & b\lambda^2 & 1 \end{pmatrix} \quad , \quad c \approx \frac{2a^2}{3b^2} \text{ or } \frac{4a^2}{3b^2} \quad , \quad (32)$$

$$\mathbf{T}_d^{1)} = \begin{pmatrix} 0 & g\lambda^3 & 0 \\ g\lambda^3 & i\hat{j}\lambda^2 & 0 \\ 0 & j\lambda^2 & 1 \end{pmatrix} \quad , \quad \mathbf{T}_d^{2)} = \begin{pmatrix} 0 & \hat{g}\lambda^3 & 0 \\ \frac{\hat{g}}{\sqrt{2}}\lambda^3 & i\hat{j}\lambda^2 & i \\ i\frac{\hat{g}}{\sqrt{2}}\lambda^3 & 0 & 1 \end{pmatrix} \frac{1}{\sqrt{2}}$$

where $\hat{g} = \sqrt{2}g$, $\hat{j} = 2j$ and $r_u \approx 1/3$. Notice that \mathbf{T}_u has two parameters and a suitable zero filling in the 11 element. In both cases \mathbf{T}_d has two parameters, its elements are

¹² We choose $n = 0$ although the data only give a limit $n \leq O(\lambda^3)$.

either real or purely imaginary. These sets of textures are thus predictive¹³ and induce in particular

$$\alpha \simeq \frac{\pi}{2} \quad , \quad \tan \beta \simeq \sqrt{\frac{1}{r_u} \frac{m_u}{m_c} \frac{m_s}{m_d}} \quad . \quad (33)$$

It is immediate to realize that $\mathbf{T}_d^{(1)}$ and $\mathbf{T}_d^{(2)}$ differ by a unitary matrix containing $R_{23}(\theta_{23} = \pi/4)$:

$$\mathbf{T}_d^{(2)} = \begin{pmatrix} 1 & 0 & 0 \\ 0 & \frac{1}{\sqrt{2}} & \frac{i}{\sqrt{2}} \\ 0 & \frac{i}{\sqrt{2}} & \frac{1}{\sqrt{2}} \end{pmatrix} \mathbf{T}_d^{(1)} \quad . \quad (34)$$

This is reflected in the magnitude of the angle $\theta_{23}^{d_R}$, which is respectively zero and maximal, while the remaining non-vanishing angles are directly related to ratios of eigenvalues

$$1) \quad s_{23}^{d_R} = 0 \quad , \quad 2) \quad s_{23}^{d_R} = \frac{1}{\sqrt{2}} \quad , \quad (35)$$

$$s_{23}^{u_L, u_R} \simeq \sqrt{\frac{m_c}{m_t}} \quad , \quad s_{23}^{d_L} \simeq \frac{m_s}{m_b} \quad , \quad s_{12}^{u_L, u_R} \simeq \sqrt{\frac{1}{r_u} \frac{m_u}{m_c}} \quad , \quad s_{12}^{d_L, d_R} \simeq \sqrt{\frac{m_d}{m_s}} \quad . \quad (36)$$

From fig. 4, it is straightforward to fit the well known CKM angles and phase to predict the less known mass ratios. Although the up, down and strange quark masses are not known with great accuracy, there is one relation among the three masses [26] which is accurately known, $1 = \frac{1}{Q^2} \frac{m_s^2}{m_d^2} + \frac{m_u^2}{m_d^2}$. Calculations based on CPT [19] find for the ellipse parameter $Q = 22.7 \pm 0.8$. A good fit of the textures in (32) is achieved with

$$\frac{m_s}{m_b} \lambda^{-2} \simeq j = 0.419 \quad , \quad \sqrt{\frac{m_d}{m_s} \frac{m_s}{m_b}} \lambda^{-3} \simeq g = 0.41 \quad , \quad (37)$$

$$\sqrt{\frac{m_c}{m_t}} \lambda^{-2} \simeq b = 1.23 \quad , \quad \sqrt{\frac{1}{r_u} \frac{m_u}{m_c} \frac{m_c}{m_t}} \lambda^{-6} \simeq a = 2.58 \quad , \quad c = 3.48 \quad .$$

To have for instance $\tan \beta = 10$ we also choose $y_t = 0.99$, $y_b = 0.17$. Fig. 5 allows for a quick check of the goodness of the fit (central values and σ 's are collected in the appendix): the listed observables are predicted to depart less than 1σ from their central value, but for $|V_{td}/V_{ts}|$ and α - hence also γ - which are a little bit beyond. In particular, according to both direct measurement [13] and recent CKM fits [14, 15], the central value of α is close to 98° . Future sensitive measurements of this angle will clarify whether the unitarity triangle is actually rectangle, thus supporting the textures in eq. (32) and their simple way of introducing CP violation.

¹³Strictly speaking there are two prediction, since eight observables (4 mass ratios and the 3+1 parameters of the CKM) are reproduced starting from five real numbers and one maximal phase.

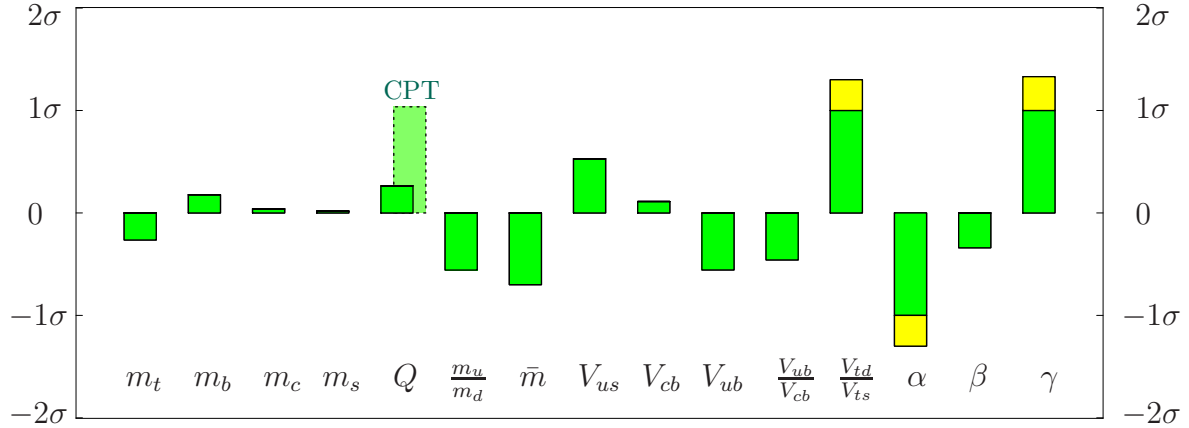


Figure 5: Predictions of textures in eq. (32) with $y_t = 0.99$, $y_b = 0.17$ ($\tan \beta = 10$) and the coefficients of eq. (37). For quark masses we use the PDG intervals [17] while for CKM we adopt the fit of [14] - see appendix for details. Explicitly, we obtain $Q = 23.5$, consistent within 1σ with the result of CPT [19] (dashed bar).

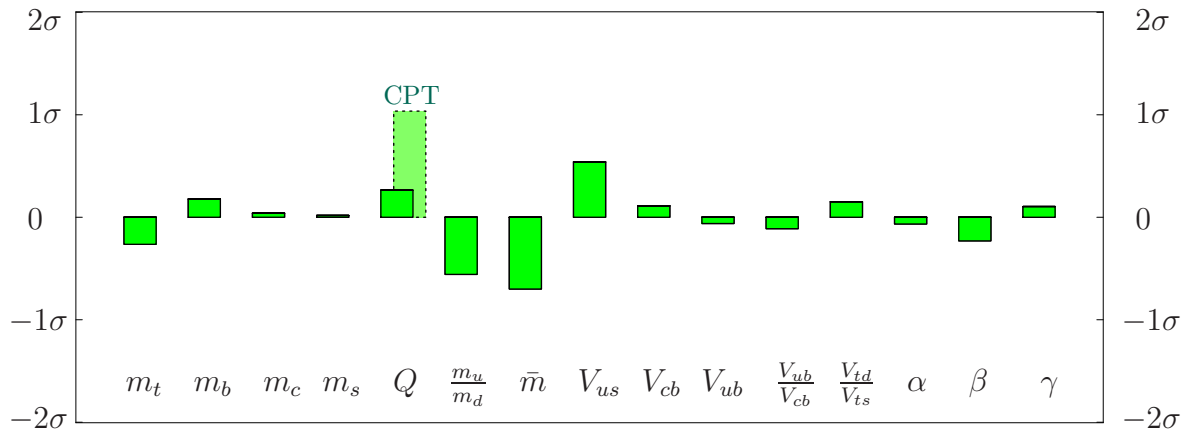


Figure 6: Same as fig. 5, but with $e^{i\phi_m} m \lambda^3 = i 0.05 \lambda^3$ as the 31-element of $\mathbf{T}_d^{1)}$.

On the contrary, if in future α will turn out to be incompatible with rectangle, the textures in eq. (32) require a proper modification, which we now turn to implement through $\mathbf{T}_d^{(1)}$ - but it is straightforward to do the same for $\mathbf{T}_d^{(2)}$, given eq. (34). The discussion in Section 3.2 suggests to exploit the correction induced by $s_{13}^{d_L} \neq 0$ with $\delta^{d_L} = \pi$ in order to enhance α without altering β . For $\mathbf{T}_d^{(1)}$, these two conditions imply $m \neq 0$ and $\phi_m = \pi/2$. In this way $\xi_t = 0$, β is practically unaffected with respect to eq. (33) while

$$\alpha \simeq \frac{\pi}{2} + \xi_b \quad , \quad \tan \xi_b = \frac{m}{g} \frac{m_s/m_b}{\tan \beta |V_{cb}|} \sim \frac{m}{g} \quad , \quad (38)$$

$$\left| \frac{V_{td}}{V_{ts}} \right| \simeq \sqrt{\frac{m_d}{m_s}} (1 - \tan \xi_b \tan \beta) \quad , \quad \left| \frac{V_{ub}}{V_{cb}} \right| \simeq \sqrt{\frac{1}{r_u} \frac{m_u}{m_c}} |1 - i \tan \xi_b| \quad .$$

One needs $\xi_b \sim 9^\circ$, namely $m/g \sim 0.12$ to reach the central value of α , in which case the negative correction to $|V_{td}/V_{ts}|$, $\tan \xi_b \tan \beta \sim 7\%$, brings it close to the central value too. On the contrary, the correction to $|V_{ub}/V_{cb}|$, $\tan^2 \xi_b \sim 2\%$, is positive and mild.

For a direct comparison with the fit of fig. 5, we keep the same values as in eq. (37) with, in addition, $e^{i\phi_m} m \lambda^3 = i 0.05 \lambda^3$ as the 31-element of $\mathbf{T}_d^{(1)}$. As shown in fig. 6, the fit to α , γ and $|V_{td}/V_{ts}|$ is further improved, while the other observables do not change significantly. Notice that, due to the smallness of m , the power of λ associated to the element $\mathbf{T}_{d31}^{(1)}$ is actually 5, rather than 3. In a flavour theory, such a small correction to the leading structure is likely to follow as a sub-leading effect.

5 Textures at M_{GUT}

We now consider the textures for \mathbf{m}_u and \mathbf{m}_d at M_{GUT} , the scale where they are presumably to be defined in view of a flavour theory. The textures of eq. (32) are defined at $M_{GUT} = 2 \times 10^{16}$ GeV in the supersymmetric grand unified context and have to be run down to m_Z to be compared to the experimental data, as we have done in the previous section. The third family Yukawa couplings dominate in the renormalization group equation and of course they affect the textures to some extent.

We have studied this effect that can be summarized as follows:

- 1) for small $\tan \beta$, in which case the top quark coupling dominates, these changes are such to affect the textures and to slightly worsen the quality of the fit, in particular for $|V_{cb}|$ which tends to be quite small;
- 2) for larger values of $\tan \beta$ the contribution due to the running of bottom and τ lepton couplings - assumed to be equal at M_{GUT} - corrects the effect due to the top coupling

$\tan \beta = 5$	y_t	y_b	\mathbf{T}_u	$\mathbf{T}_d^{1)}$
M_{GUT}	0.61	0.028	$\begin{pmatrix} -3.70\lambda^8 & 1.84\lambda^6 & 0 \\ 1.84\lambda^6 & 0 & 1.03\lambda^2 \\ 0 & 1.03\lambda^2 & 1 \end{pmatrix}$	$\begin{pmatrix} 0 & 0.33\lambda^3 & 0 \\ 0.33\lambda^3 & i 0.34\lambda^2 & 0 \\ 0 & 0.34\lambda^2 & 1 \end{pmatrix}$
m_Z	1.00	0.086	$\begin{pmatrix} -5.49\lambda^8 & 2.73\lambda^6 & O(\lambda^8) \\ 2.73\lambda^6 & -0.51\lambda^4 & 1.03\lambda^2 \\ O(\lambda^8) & 1.03\lambda^2 & 1 \end{pmatrix}$	$\begin{pmatrix} O(\lambda^{15}) & 0.38\lambda^3 & O(\lambda^7) \\ 0.38\lambda^3 & i 0.39\lambda^2 & O(\lambda^6) \\ O(\lambda^9) & 0.24\lambda^2 & 1 \end{pmatrix}$

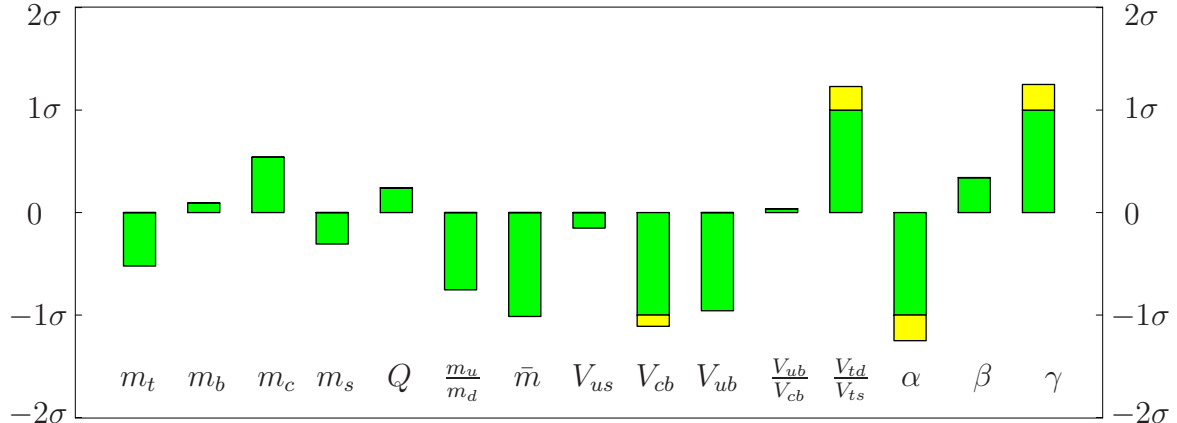


Figure 7: Predictions of the textures above with $\tan \beta = 5$ faced to experimental data. For quark masses we use the PDG intervals [17] while for CKM we adopt the fit of [14]. The ellipse parameter Q is consistent within 1σ with the CPT result [19].

enough to allow a good fit to the data. Therefore, the model prefers values of $\tan \beta$ above 15.

Using the 1-loop renormalization group equations, we have carried out a quantitative study of the quark textures \mathbf{T}_u and $\mathbf{T}_d^{1)}$ for the two representative cases $\tan \beta = 5$ and $\tan \beta = 35$. In both cases, we display the textures at M_{GUT} , where they are naturally defined, and show how they are modified at low energy, where quark masses and the CKM matrix elements are measured. As can be seen from figs. 7 and 8, experimental data are well reproduced. Since the angles of the unitarity triangle are mildly affected by the running (independently of the value of $\tan \beta$), the typical signature of our proposed

$\tan \beta = 35$	y_t	y_b	\mathbf{T}_u	\mathbf{T}_d^1
M_{GUT}	0.61	0.233	$\begin{pmatrix} -3.60\lambda^8 & 1.77\lambda^6 & 0 \\ 1.77\lambda^6 & 0 & 1.01\lambda^2 \\ 0 & 1.01\lambda^2 & 1 \end{pmatrix}$	$\begin{pmatrix} 0 & 0.32\lambda^3 & 0 \\ 0.32\lambda^3 & i 0.33\lambda^2 & 0 \\ 0 & 0.33\lambda^2 & 1 \end{pmatrix}$
m_Z	0.99	0.589	$\begin{pmatrix} -5.47\lambda^8 & 2.69\lambda^6 & O(\lambda^8) \\ 2.69\lambda^6 & -0.50\lambda^4 & 1.01\lambda^2 \\ O(\lambda^8) & 1.01\lambda^2 & 1 \end{pmatrix}$	$\begin{pmatrix} O(\lambda^{15}) & 0.40\lambda^3 & O(\lambda^7) \\ 0.40\lambda^3 & i 0.41\lambda^2 & O(\lambda^6) \\ O(\lambda^9) & 0.24\lambda^2 & 1 \end{pmatrix}$

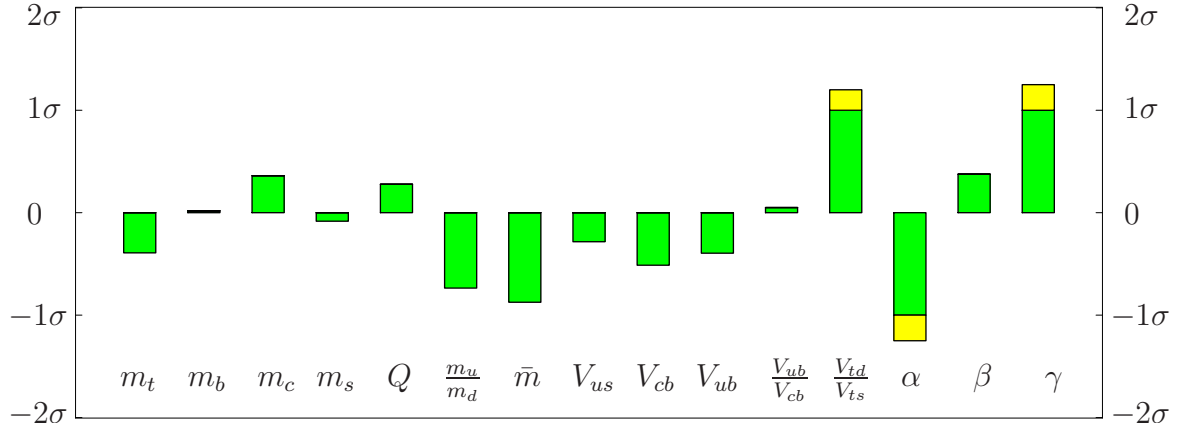


Figure 8: Predictions of the textures above with $\tan \beta = 35$ faced to experimental data. For quark masses we use the PDG intervals [17] while for CKM we adopt the fit of [14]. The ellipse parameter Q is consistent within 1σ with the CPT result [19].

textures, $\alpha \approx 90^\circ$, persists.

6 Extension to the Lepton Sector

The picture can now be completed by considering also the lepton sector. Embedding \mathbf{T}_d of eq. (32) in an $SU(5)$ grand unified theory, one realizes that the GJ relations $m_b = m_\tau$, $3m_s = m_\mu$ and $m_d = 3m_e$ [3], are achieved with $(g, \hat{g})_d \rightarrow (g, \hat{g})_e$ while $(j, \hat{j})_d \rightarrow (-3j, -3\hat{j})_e$, corresponding respectively to a $\bar{\underline{5}}_H$ and a $\bar{\underline{45}}_H$ (the latter could result from the insertion of a $\underline{24}_H$ or $\underline{75}_H$). With the GJ prescription, the fit of the quark

mass matrices of Section 5 leads to charged lepton masses that miss the experimental value by $O(10\%)$.

More generally, the parameters in \mathbf{T}_d and \mathbf{T}_e would get contributions from higher dimension operators that would slightly modify the GJ relations [6]. Let us decompose the values of the coefficients found in fig. 8 for $\tan\beta = 35$ in sums of $\underline{5}_H$ and $\underline{45}_H$ contributions: $g = g_5 + g_{45}$, $j = j_5 + j_{45}$, $1 = u_5 + u_{45}$. Hence, $\mathbf{T}_e^{1)T}$ has the same form of $\mathbf{T}_d^{1)}$ but with coefficients $g_5 - 3g_{45}$, $j_5 - 3j_{45}$, $u_5 - 3u_{45}$, respectively. From the fit of the charged lepton masses run down at the scale m_Z , it turns out that $g_{45}/g_5 = -3.8\%$, $j_5/j_{45} = -15.7\%$, $u_{45}/u_5 = -4.5\%$. However, it is well known that $b - \tau$ unification [21] is a very model dependent issue: there are significant low energy threshold corrections that restrict the supersymmetric parameter space and strongly depend on $\tan\beta$ [22]; also, possible high energy threshold corrections could be significant, like e.g. the seesaw or GUT ones [23]. Therefore, a detailed analysis of the extension of our textures to the charged lepton sector would only be justified in the context of a well defined supersymmetric model and a neutrino mass generation mechanism.

Supported by the fact that the charged lepton textures turn out to be quite close to the simple GJ extension, let us analyse the consequences of such prescription for mixings and CPV in the lepton sector. We write the two mass textures

$$\tilde{\mathbf{T}}_d^{1)} = \mathbf{T}_e^{1)T} = \begin{pmatrix} 0 & g\lambda^3 & 0 \\ g\lambda^3 & -3ij\lambda^2 & 0 \\ 0 & -3j\lambda^2 & 1 \end{pmatrix} \quad (39)$$

$$\tilde{\mathbf{T}}_d^{2)} = \mathbf{T}_e^{2)T} = \begin{pmatrix} 0 & \hat{g}\lambda^3 & 0 \\ \frac{\hat{g}}{\sqrt{2}}\lambda^3 & -3ij\lambda^2 & i \\ i\frac{\hat{g}}{\sqrt{2}}\lambda^3 & 0 & 1 \end{pmatrix} \frac{1}{\sqrt{2}}, \quad (40)$$

which differ by the magnitude of $\theta_{23}^{e_L}$, while the other non-vanishing mixings are small and simply related to the left-mixings of down-quarks:

$$1) \quad s_{23}^{e_L, d_R} \simeq 0 \quad , \quad 2) \quad s_{23}^{e_L, d_R} \simeq \frac{1}{\sqrt{2}} \quad , \quad (41)$$

$$\frac{m_\mu}{m_\tau} \simeq s_{23}^{e_R} = 3s_{23}^{d_L} \quad , \quad \sqrt{\frac{m_e}{m_\mu}} \simeq s_{12}^{e_L, e_R} = \frac{s_{12}^{d_R, d_L}}{3} \sim \frac{\theta_C}{3} \quad . \quad (42)$$

It is also interesting to study possible connections between CPV in quark and lepton sectors. Due to the $SU(5)$ relation $\Phi_{e_L} = -\tilde{\Phi}_{d_R}$, where the latter are the phases associated to $\tilde{\mathbf{T}}_d$, quark phases explicitly appear in the expression for U_{MNS} , eq. (6).

In case 1), one can read from eq. (24) that $\tilde{\phi}_{12}^{d_R} = \pi/2$, hence $\phi_{12}^{e_L} = -\pi/2 = -\phi_{12}^q$. Due to $\theta_{23}^{d_R, e_L} \simeq 0$, one can get rid of $\phi_{23}^{e_L}$ by proper phase redefinitions of fields. The only source of flavour violation in the charged lepton sector, $\theta_{12}^{e_L} \sim 4^\circ$, is too small to account

for the solar angle. Hence, not only the atmospheric, but also the solar angle has to come from m_ν^{eff} of eq. (1).

Case 2) is more interesting, because $\theta_{23}^{e_L}$ is maximal and so is $\phi_{23}^{e_L}$. Indeed, eqs. (24) and (25) imply $\tilde{\phi}_{12,23}^{d_R} = \pi/2$, so that

$$\phi_{12,23}^\ell + \phi_{12,23}^\nu = \phi_{12,23}^{e_L} = -\frac{\pi}{2} = -\phi_{12}^q . \quad (43)$$

If ϕ_{23}^ν is very small or close to π , the maximal phase ϕ_{23}^ℓ makes the atmospheric angle maximal independently of θ_{23}^ν [16]; namely, θ_{atm} is maximal if the maximal CPV between charged leptons is not compensated by a large CPV between the corresponding neutrinos. Since $\theta_{12}^{e_L} \sim 4^\circ$, the solar mixing angle must mainly come from m_ν^{eff} . If $\theta_{13}^\nu \simeq 0$, one has the prediction $|U_{e3}| \simeq s_{12}^{e_L}/\sqrt{2} \approx 0.05$ and the relation

$$\theta_{12}^{MNS} = \theta_{12}^\nu + |U_{e3}| \cos \delta^{MNS} . \quad (44)$$

The value $\theta_{12}^\nu = \arctan(1/\sqrt{2})$, typical for tribimaxing models [27], is particularly interesting because, in this case, the experimental value of the solar angle forces δ^{MNS} to be maximal (see fig. 3 of ref. [16]).

7 Conclusions

We have derived two sets of fermion mass matrices adopting the following guidelines:

- the least number of parameters with the highest number of vanishing elements;
- phases of the form $n\pi/2$.

The quark mass matrices with only four parameters corresponding to the four mass ratios, eqs. (13) and (14), give a reasonable fit but for m_u , which turns out too large as compared to the chiral perturbation theory value [19]. This requires the introduction of one more small parameter $O(m_u)$ which shifts this mass down, as in eq. (32). The fit shows that some matrix elements are likely to be exactly equal or just related by factors of $\sqrt{2}$, favouring the interpretation of the textures in terms of a non-abelian flavour theory.

A crucial prediction of these textures is $\alpha \approx \pi/2$. This is a consequence of our justified assumption $\theta_{13}^{d_L, u_L} = 0$. Indeed, in such a case it turns out (fig. 4) that the best choice to account for the observed CPV in the quark sector is the presence of only one maximal phase, to be identified with the non-removable phase ϕ_{12}^q .

The present direct measure suggests $\alpha = 99^\circ_{-9^\circ}^{+12^\circ}$ at 1σ [13], with a sensitivity already comparable to that of the recent fits of the CKM unitary matrix, $\alpha = 98.1^\circ_{-7^\circ}^{+6.3^\circ}$ at 1σ [14]. Interestingly enough, B physics experiments already in progress will significantly improve the sensitivity to α in a few years. Such experiments will provide a crucial test of these textures. If in future α will stay close to its present central value but its sensitivity will

allow to exclude $\alpha = \pi/2$, a suitable modification makes the textures still viable. This is achieved for instance by filling the 31-element of \mathbf{T}_d^1 with an additional purely imaginary small parameter, of $O(\lambda^5)$. In the case that α will turn out to be considerably larger than its present central value, the model requires more than just a small correction.

A large value of $\tan \beta$ is slightly preferred because in the running from M_{GUT} down to m_Z the effect of the contribution of the top coupling deteriorates the fit of $|V_{cb}|$, which can be corrected by the bottom and τ contributions to the running. We have provided explicit numerical examples of our proposed textures at M_{GUT} for two representative values of $\tan \beta$, figs. 7 and 8.

Leptons have been incorporated in the analysis in the framework of an $SU(5)$ GUT by a generalisation of the GJ mechanism, via the insertion of an $SU(5)$ breaking v.e.v. in the element of \mathbf{T}_d which bears the maximal phase inducing $\alpha \approx \pi/2$. The quark and lepton CPVs would then have a common origin, further related to $SU(5)$ breaking. The known phase δ in the CKM, which is known not to be suitable for baryogenesis is related to a phase in the lepton mass matrices that could be operative in leptogenesis.

At a more theoretical side, the obvious question is whether these textures are naturally understood, namely whether they can be derived in a flavour theory. It turns out that there is a relatively simple model which can explain and even relate the parameters in the textures [28].

Acknowledgements

I.M. thanks G. Altarelli for useful discussions. We thank the Dep. of Physics of Rome1 and the CERN for hospitality during the completion of this work. This project is partially supported by the RTN European Program MRTN-CT-2004-503369.

Appendix: Input data

We collect below intervals (central values in the middle) at 1 and 2σ extracted from the CKM fit or ref. [14] at m_Z :

$ V_{us} $	(.22422, .22523, .22625, .22723, .22823)
$ V_{cb} $	(.04047, .04131, .04224, .04267, .04310)
$ V_{ub} $	(.003708, .003804, .003899, .004001, .00415)
$ V_{td}/V_{ts} $	(.1717, .1884, .1982, .2095, .2243)
$ V_{ub}/V_{cb} $	(.0874, .0899, .0923, .0955, .0994)
R_u	(.377, .387, .398, .409, .424)
γ	(43.5, 52.7, 58.6, 65.4, 74.3)
β	(21.10, 22.45, 23.22, 23.96, 24.92)
α	(82.4, 91.1, 98.1, 104.4, 114.9)

Using the PDG [17] values and the multiplicative factors to go to m_Z collected below,

	PDG at 1σ [17]	CPT [19]	factor to go to m_Z [11]
$m_t(\text{pole})$	172.7 ± 2.9 GeV		
$m_t(m_t)$	163.5 ± 2.8 GeV		1.06
$m_b(m_b)$	4.25 ± 0.15 GeV		0.69
$m_c(m_c)$	1.3 ± 0.10 GeV		0.56
$m_s(2\text{GeV})$	105 ± 25 MeV		0.65
$m_d(2\text{GeV})$	$4 - 8$ MeV		0.65
$m_u(2\text{GeV})$	$1.5 - 4$ MeV		0.65
$\bar{m}(2\text{GeV})$	$3 - 5.5$ MeV		0.65
$Q = \frac{m_s/m_d}{\sqrt{1-(m_u/m_d)^2}}$	$21 - 25$	22.7 ± 0.8	
m_u/m_d	$0.3 - 0.7$	0.553 ± 0.043	
m_s/m_d	$17 - 22$	18.9 ± 0.8	

we obtain the following intervals (central values in the middle) for mass ratios at m_Z :

$$\begin{aligned}
 \frac{m_c}{m_t} &= (3.81, 4.20, 4.60) \times 10^{-3} & \frac{m_s}{m_b} &= (1.71, 2.33, 2.99) \times 10^{-2} & , \\
 \frac{m_c}{m_s} &= (7.95, 10.67, 15.08) & \frac{m_d}{m_s} &= (.046, .051, .059) & , & \frac{m_u}{m_c} &= (0.91, 2.4, 5.2) \times 10^{-3} & .
 \end{aligned} \tag{45}$$

References

[1] R. Gatto, G. Sartori and M. Tonin, Phys. Lett. **B28** (1968) 128; N. Cabibbo, L. Maiani, Phys. Lett. **B28** (1968) 131. See also: R.J. Oakes, Phys. Lett. **B29** (1969) 683; S. Weinberg in *A Festschrift for I.I. Rabi*, ed. by L. Motz, New York 1977; F. Wilczek and A. Zee, Phys. Lett. **70B** (1977) 418.

- [2] H. Fritzsch, Phys. Lett. **70B** (1977) 436; Phys. Lett. **73B** (1978) 317.
- [3] H. Georgi and C. Jarlskog, Phys. Lett. **86B** (1979) 297. See also: J. Harvey, P. Ramond, D. Reiss, Phys. Lett. **B92** (1980) 309; S. Dimopoulos, L.J. Hall and S. Raby, Phys. Rev. Lett. **68** (1992) 1984; S. Dimopoulos, L.J. Hall and S. Raby, Phys. Rev. **D45** (1992) 4192.
- [4] P. Ramond, R.G. Roberts and G.G. Ross, Nucl. Phys. **B406** (1993) 19.
- [5] L. Hall and A. Rasin, Phys. Lett. **B315** (1993) 164, hep-ph/9303303.
- [6] R. Barbieri, L.J. Hall, S. Raby and A. Romanino, Nucl. Phys. **B493** (1997) 3, hep-ph/9610449; R. Barbieri, L.J. Hall and A. Romanino, Phys. Lett. **B401** (1997) 47, hep-ph/9702315; Nucl. Phys. **B551** (1999) 93, hep-ph/9812384.
- [7] H. Fritzsch and Z.Z. Xing, Phys. Lett. **B 413** (1997) 396, hep-ph/9707215. See also: H. Fritzsch and Z.Z. Xing, Phys. Lett. **B 353** (1995) 114, hep-ph/9502297.
- [8] H. Fritzsch and Z.Z. Xing, Phys. Lett. **B 506** (2001) 109, hep-ph/0102295.
- [9] R.G. Roberts, A. Romanino, G.G. Ross and L. Velasco-Sevilla, Nucl. Phys. **B615** (2001) 358, hep-ph/0104088.
- [10] F. Caravaglios, P. Roudeau and A. Stocchi, Nucl. Phys. **B633** (2002) 193, hep-ph/0202055.
- [11] H.D. Kim, S. Raby and L. Schradin, JHEP 0505 (2005) 036, hep-ph/0401169.
- [12] G.C. Branco, M.N. Rebelo and J.I. Silva-Marcos, Phys. Lett. **B 597** (2004) 155, hep-ph/0403016.
- [13] For a review and references, see e.g.: Z. Ligeti, hep-lat/0601022.
- [14] The CKMfitter Group, *Updated results on the CKM matrix and the unitarity triangle, including results presented at HEP 2005*, August 1, 2005, <http://ckmfitter.in2p3.fr>
- [15] The UTfit Collaboration, M. Bona et al., hep-ph/0509219; M. Bona et al., JHEP 0507 (2005) 028, hep-ph/0501199.
- [16] I. Masina, Phys. Lett. **B 633** (2006) 134, hep-ph/0508031.
- [17] Review of Particle Physics, S. Eidelman et al., Phys. Lett. **B 592** (2004) 1. See also: K. Hagiwara et al., Phys. Rev. **D 66** (2002) 010001; D.E. Groom et al, The European Physical Journal **C 15** (2000) 1.

- [18] H. Fritzsch and Z. Xing, hep-ph/0601104.
- [19] H. Leutwyler, Phys. Lett. **B378** (1996) 313, hep-ph/9602366; Nucl. Phys. Proc. Suppl. 94 (2001) 108, hep-ph/0011049.
- [20] H. Georgi, S.L. Glashow, Phys. Rev. Lett. **32** (1974) 438.
- [21] M. Chanowitz, J. Ellis, M.K. Gaillard, Nucl. Phys. **B 128** (1977) 506; A. Buras, J. Ellis, M.K. Gaillard, D.V. Nanopoulos, Nucl. Phys. **B 135** (1978) 66.
- [22] L.J. Hall, R. Rattazzi, U. Sarid, Phys. Rev. **D 50** (1994) 7048; R. Hempfling, Phys. Rev. **D 49** (1994) 6168; M. Carena, M. Olechowski, S. Pokorski and C.E.M. Wagner, Nucl. Phys. **B 426** (1994) 269; J. Bagger, K. Matchev and D. Pierce, Phys. Lett. **B 348** (1995) 443;
- [23] A. Brignole, H. Murayama and R. Rattazzi, Phys. Lett. **B 335** (1994) 345; F. Vissani and A.Y. Smirnov, Phys. Lett. **B 341** (1994) 173; G.K. Leontaris, S. Lola and G.G. Ross, Nucl. Phys. **B 454** (1995) 25; A. Dedes and K. Tamvakis, Phys. Rev. **D 56** (1997) 1496, hep-ph/9703374.
- [24] G.L. Fogli, E. Lisi, A. Marrone and A. Palazzo, hep-ph/0506083. See also: M.C. Gonzalez-Garcia, M. Maltoni and A. Yu. Smirnov, Phys. Rev. **D 70** (2004) 093005, hep-ph/0408170.
- [25] L. Wolfenstein, Phys. Rev. Lett. **51** (1983) 1945.
- [26] See, for example, the PDG article on quark masses by Manohar and Sachrajda or: D.B. Kaplan and A.V. Manohar, Phys. Rev. Lett. **56** (1986) 2004; H. Leutwyler, the first ref. in [19].
- [27] P.F. Harrison, D.H. Perkins, W.G. Scott, Phys. Lett. **B458** (1999) 79, hep-ph/9904297; Phys. Lett. **B530** (2002) 167, hep-ph/0202074.
- [28] I. Masina and C.A. Savoy, hep-ph/0606097.